Asian Journal of Chemistry; Vol. 33, No. 10 (2021), 2400-2410

ASIAN JOURNAL OF CHEMISTRY

https://doi.org/10.14233/ajchem.2021.23351

Spectral and Electrochemical Sensing Studies of Unsymmetrical Schiff Bases having Enhanced Antifungal Activity

SELVARAJ SHUNMUGAPERUMAL[1], SARANYA DHASARATHAN[1], KAMATCHI SELVARAJ P[1,*], ILANGO KALIAPPAN[2] and BATHULA SIVA KUMAR[2]

[1]PG & Research Department of Chemistry, Government Arts College for Men (Autonomous), Nandanam, Chennai-600035, India
[2]Department of Pharmaceutical Chemistry, SRM College of Pharmacy, SRM Institute of Science and Technology, Kattankulathur-603203, India

*Corresponding author: E-mail: porbal96@gmail.com

Received: 2 June 2021; *Accepted*: 27 July 2021; *Published online*: 20 September 2021; AJC-20513

Novel unsymmetrical Schiff bases comprising azomethine spin-off having ferrocene moiety at one end and simple aromatic component attached imine at other end, capable of sensing multiple metal ions have been synthesized. The MLCT charge transfer band in UV-Visible studies upon coordination with metal ions with receptors is recorded particularly for Cu^{2+} ions. The observed ΔE_p values with change in scan rate for metal free and metal added receptor solution suggest quasi-reversible process. Agar well diffusion method and molecular docking studies reveals that the synthesized compounds inhibit more efficiently fungi rather than bacteria, which hampers the progress of microbial research, as the available antifungal agents are minimal compared to antibacterial counterpart.

Keywords: Unsymmetrical Schiff bases, Azomethine, Ferrocene, Cation sensors, Binding attitude, Molecular docking.

INTRODUCTION

Toxic impact of transition and heavy metal ions in chemical, biological and environmental fields secured greatest importance since such ions played a significant role on the environment and human health [1]. Tedious and several hours consuming detections techniques like atomic absorption spectrometry, high-performance liquid chromatography, mass spectrometry, and atomic emission spectrometry are engaged to detect toxic pollutants [2]. Dramatis personae of chemosensor projected them to unique attitude, considering their short response time, ability to give on-site ascertainment and immense selectivity and sensitivity [3]. Applications of chemosensors in diverse field apart from industrial applications [4] acquiring captivated prevalent interest encompassed by the scientific community. Many groups have succeeded in developing selective, sensitive and multi-functional chemosensors for health and environmental destroying hazardous heavy metal ions [1-5].

Determination of toxins and metal ions have been studied using Schiff base, considering the easy synthesis and their simplicity in complex formation with metal ions [6]. Selectivity of specific metal ions mostly depends upon the size of the ion, hard-soft acid base nature of donor atom of the sensor and metal ions [7]. Nucleophilic addition of amines and carbonyl compounds give hemiaminal which on dehydration bring about Schiff base having >C=N- group [8]. Ample amount of chemosensors with ferrocene moiety have been broadly developed due to exceptional sensitivity, stability, redox activity and excellence *in vitro* cytotoxic effect [9,10].

Important organs of the body like brain, liver, kidney and immune system suffered irrecoverable damages by the accumulation of Hg^{2+} concentration greater than 10 nM [11]. Neurotoxicity, mitochondrial dysfunctions and oxidative stress have been reported for the greater consumption of Ni^{2+} ions [12]. Copper ions are essential for many biological activities including cellular energy production, transduction of signals and oxygen transfer mechanism [13]. Excess intake of Cu^{2+} ions concentration beyond 1.3 mg/L along with drinking water [14] exchange the nutrient minerals from enzymes [15], which in turn alters the functions of many enzymes [16].

Longer biological half-life period of Cd^{2+} makes it a cumulative toxin and that affects lung, induces renal and prostate cancer along with calcium metabolism disorder [17]. Up keeping the levels of blood sugar, vitamins, immune cell function and

nerve system in biological organisms is associated with Mn^{2+} concentration [18]. Reduced level of Mn^{2+} ions in human blood breed bone modeling osteoporosis and neurological system related to epileptics [19]. Exorbitance level of Mn^{2+} leads to neurodegenerative damage resulting in Parkinson's disease [20]. Toxicity of lead causes acute change in biological oxygen carrier process, enhance blood pressure, weakness at bone joint, reduction of fertility in male and prevent brain development in children [21].

Present work focus upon the synthesis of the novel schiff base N′^{1}-((*E*)-ferrocenylidene)-N′^{3}-((*E*)-4-nitrobenzylidene)-malonohydrazide and N′^{1}-((*E*)-ferrocenylidene)-N′^{3}-((*E*)-4-*N*,*N*-dimethylaminobenzylidene)malonohydrazide compound having ferrocene moiety at one end of the central back bone and simple aromatic component at the other end. The newly synthesized chemosensors show affinity and sensing tendency towards multiple metal ions like Ni^{2+}, Cu^{2+}, Mn^{2+}, Hg^{2+}, Cd^{2+} and Pb^{2+}. The nitrogen donor of the Schiff base ligand with sp^2 hybridized orbital is responsible for ample chemical and biological activities of azomethine moiety [22]. The active center of the cell makes hydrogen bond with the nitrogen donor of the azomethine groups, which affect the cell process and develops antibacterial, antifungal and anticancer activities [23]. Compared to antifungal compounds enormous amount of antibacterial mixtures have been reported [24]. The newly synthesized sensor exhibits better antifungal activity rather than antibacterial activities.

EXPERIMENTAL

Analytical grade of hydrazine hydrate, dimethylmalonate, 4-nitrobenzaldehyde, *p*-dimethylaminobenzaldehyde, ferrocene carboxaldehyde and silica gel were purchased from E. Merck and used without further purification. Metal salts *viz*. $MnCl_2$, $NiCl_2$, $HgCl_2$, $CuCl_2$, $Cd(OAc)_2$ and $Pb(OAc)_2$ used in the spectrophotometric and cyclic voltammetry studies were of analytical grade and procured from Sigma-Aldrich. Tetrabutylammonium perchlorate of < 99% was acquired from Chemical Center, India and used as received. Spectroscopy grade absolute ethanol obtained from Commercial Alcohols, Canada and HPLC grade acetonitrile (E-Merck) were used for spectral studies.

Mass spectra were recorded on Bruker Daltonics esquire 3000 spectrometer. Nuclear magnetic resonance (^{1}H NMR) spectra were documented on a 500 MHz, Bruker Avance spectrometer engaging C_2D_5OD as solvent. FTIR spectra were carried out in Perkin-Elmer 337 spectrometer in the range of 4000-400 cm^{-1} using KBr pellets. UV-visible spectral studies were conducted on Shimadzu Model UV-1800 240V spectrophotometer between 200 and 800 nm. Cyclic voltammograms were registered on CHI electrochemical analyzer 1200B model having glassy carbon as working electrode, platinum as counter electrode and Ag/AgCl as reference electrode. Tetrabutylammonium perchlorate solution having 0.1M concentration was used as supporting electrolyte and all measurements were carried out in nitrogen atmosphere. The C, H and N contents were analyzed with Perkin-Elmer 2400 series CHSN/O Analyser.

Synthesis of *N*′^{1}-((*E*)-ferrocenylidene)-*N*′^{3}-((*E*)-4-nitrobenzylidene)malonohydrazide (R1): Diethyl malonate (1 mol) and hydrazine hydrate (2 mol) were allowed to react to generate malonyldihydrazide [25]. To a clear solution of purified malonyldihydrazide (0.01 mol) dissolved in 50 mL ethanol, a mixture of 4-nitrobenzaldehyde (0.01 mol) and ferrocenecarboxaldehyde (0.01 mol) in 150 mL ethanol was added and stirred for 0.5 h and then refluxed for 6-7 h. Cooled reaction mixture was filtered and concentrated to get dark reddish orange coloured *N*′^{1}-((*E*)-ferrocenylidene)-*N*′^{3}-((*E*)-4-nitrobenzylidene)malonohydrazide (**Scheme-I**). The crude sample was purified in a column having silica gel as stationary phase. Ethanol was used as eluent. Yield: 0.4614 g (99%), m.p.: 80 ºC. Anal. calcd. (found) (%) of $C_{21}H_{19}N_5O_4Fe$: C, 54.78 (54.72); H, 4.13 (4.10); N, 15.21 (15.18); O, 13.91 (13.72).

Synthesis of *N*′^{1}-((*E*)-ferrocenylidene)-*N*′^{3}-((*E*)-4-*N*,*N*-dimethylaminobenzylidene)malonohydrazide (R2): Blend having malonyldihydrazide (0.01 mol) in 50 mL of ethanol, 0.01 mole of *p*-dimethylaminobenzaldehyde and 0.01 mol of ferrocenecarboxaldehyde in 150 mL ethanol was stirred for 0.5 h and refluxed for 6-7 h (**Scheme-I**). Isolation of compound *N*′^{1}-((*E*)-ferrocenylidene)-*N*′^{3}-((*E*)-4-*N*,*N*-dimethylaminobenzylidene)malonohydrazide (R2) was carried out adopting the same procedure used for compound R1. Colour: dark reddish orange. Yield: 0.5341 g (87%), m.p.: 90 ºC. Anal. calcd. (found) (%) of $C_{21}H_{19}N_5O_2Fe$: C, 52.94 (52.90); H, 3.99 (3.95); N, 14.70 (14.68); O, 16.80 (16.76).

Antimicrobial activity: Antimicrobial activity (*in vitro*) of the synthesized ligands was done by standard method [26]

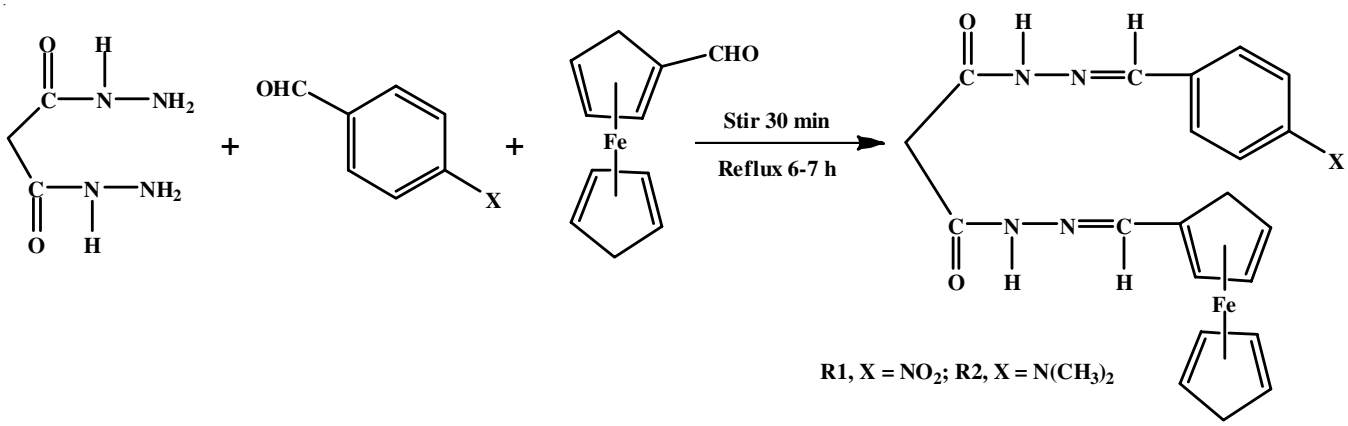

Scheme-I

against two Gram-positive (*Staphylococcus aureus* and *Streptococcus faecalis*), two Gram-negative (*Escherichia coli* and *Salmonella typhimurium*) bacteria at 37 ºC and two fungi (*Candida albicans* and *Aspergillus niger*) at room temperature. The tests were carried out in triplicate and the average values were considered for analysis.

Molecular docking studies: Docking study was performed for the synthesized compounds R1 and R2 using Autodock 4.2.6 [27] running on windows 7, to investigate their binding mode with the target protein. Enzyme used for the docking study was retrieved from RCSB, Protein Data Bank (PDB). MGL tools of Autodock were used for preparation of target protein. The structures of the synthesized compounds R1 and R2 were drawn using ChemSketch and converted to 3D structure with the help of 3D optimization tool. By using ligand module, the drawn ligands were geometrically optimized; partial atomic charges were computed using MMFF94 force field. Prepared ligands were docked with preferred protein using Autodock tools. The best docked pose obtained from Autodock was analyzed.

RESULTS AND DISCUSSION

Mass spectral studies: Appearance of molecular peak (ESI) *m/z* at 460 and 458 for *N*′^{1}-((*E*)-ferrocenylidene)-*N*′^{3}-((*E*)-4-nitrobenzylidene)malonohydrazide and *N*′^{1}-((*E*)-ferrocenylidene)-*N*′^{3}-((*E*)-4-*N*,*N*-dimethylaminobenzylidene)malonohydrazide, respectively on mass spectral analysis confirmed the formation of expected receptors.

FTIR studies: The FTIR spectral peaks of compound R1 observed around 457 cm^{-1} is pertinent to tilt stretching vibration of ferrocene cyclopentadienyl ring and the peak positioned at 826 cm^{-1} corresponds to C-H out of plane bend vibration. The peaks appeared between 991 to 1240 cm^{-1} related to the -C-C-H bending vibration in the cyclopentadienyl ring [28]. The peaks at 1341, 1516 and 1653 cm^{-1} are assigned for the symmetric stretching vibrations of -NO_2, -CH=N (imine) stretching vibration and amide -C=O stretching vibration, respectively [29]. The characteristic peaks at 3090 and 3200 cm^{-1} are attributed to the stretching vibration of secondary amine and water of hydration (Fig. 1). Compound R2 also give the above mentioned peaks along with stretching vibrational modes in CH_3 groups around 2896 cm^{-1} [30].

NMR studies: ^{1}H NMR spectrum of compound R1 in C_2D_5OD solvent contains the relevant peaks and are assigned accordingly δ (ppm): 8.1(s, 2H, NCH), 7.4 (m, 2H, aromatic), 6.7 (d, 2H, aromatic), 4.7 (m, 2H, cp substituted), 4.5 (m, 2H, cp substituted), 4.2 (s, 5H, cp unsubstituted), 1.19 (s, 2H, 2NH) (Fig. 2). Alike spectral peaks along with a prominent singlet at δ 3.7 (6H) due to two N-methyl protons is observed for compound R2.

Incorporation of metal ions: The metal salts $CuCl_2$, $HgCl_2$ and $NiCl_2$ are soluble in acetonitrile whereas $MnCl_2$, $Pb(OAc)_2$ and $Cd(OAc)_2$ are soluble in ethanol. The difference in solubility splits the sensing studies into two parts. Acetonitrile solution for first set and alcoholic solution for second set were used. Compound R1 shows a shoulder around 241 nm and high energy band at 295 nm in ethanol (Fig. 3a). In acetonitrile a slight bend near 245 nm and high energy band at 292 nm was

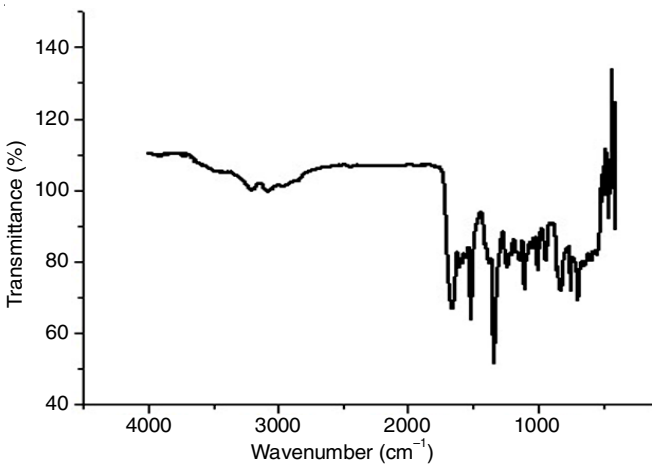

Fig. 1. FTIR spectrum of R1

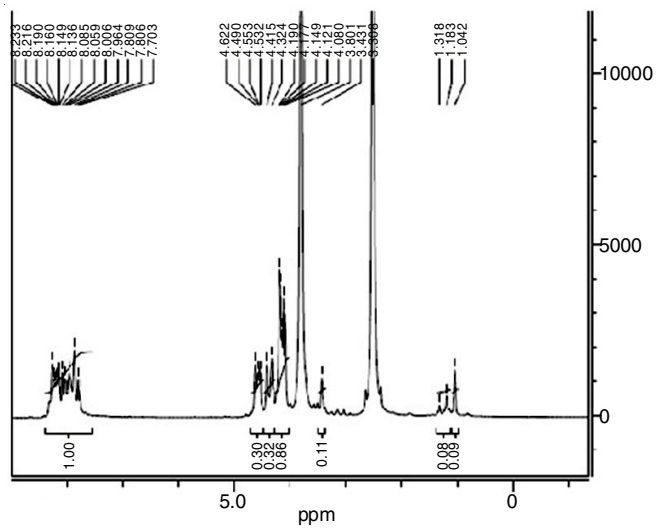

Fig. 2. ^{1}H NMR spectrum of R1

observed for compound R1 (Fig. 3b). These observations are assigned to π-π* transition of aromatic ring [5]. Shoulder perceived near 329 nm is attributed to intramolecular charge transfer transition [31].

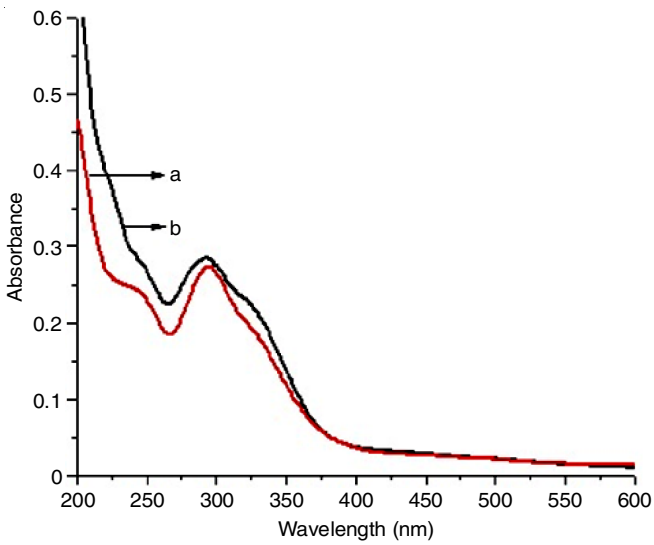

Fig. 3. UV-visible spectrum of R1 in (a) ethanol (b) acetonitrile

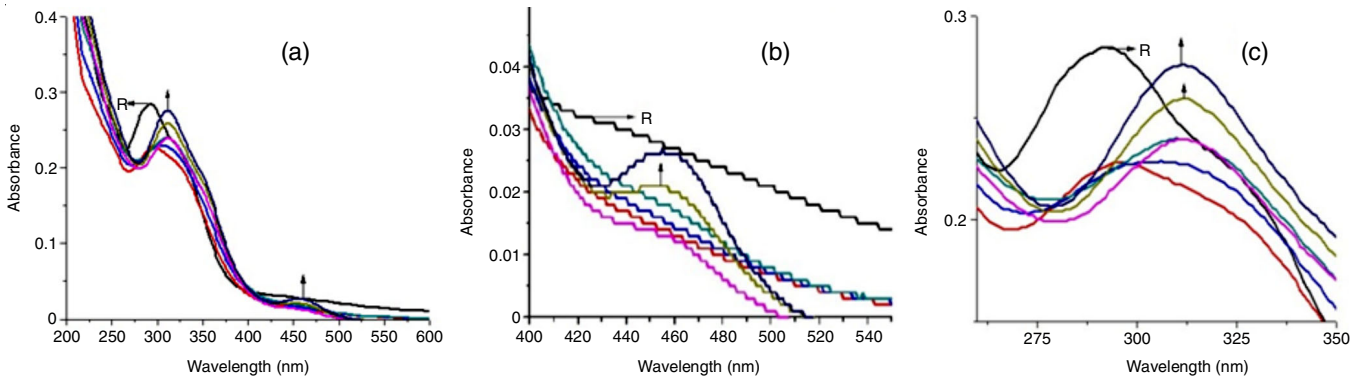

Fig. 4. Spectral changes for the addition of copper salt (a) overall changes, (b) formation of MLCT band, (c) redshift of 295 nm peak

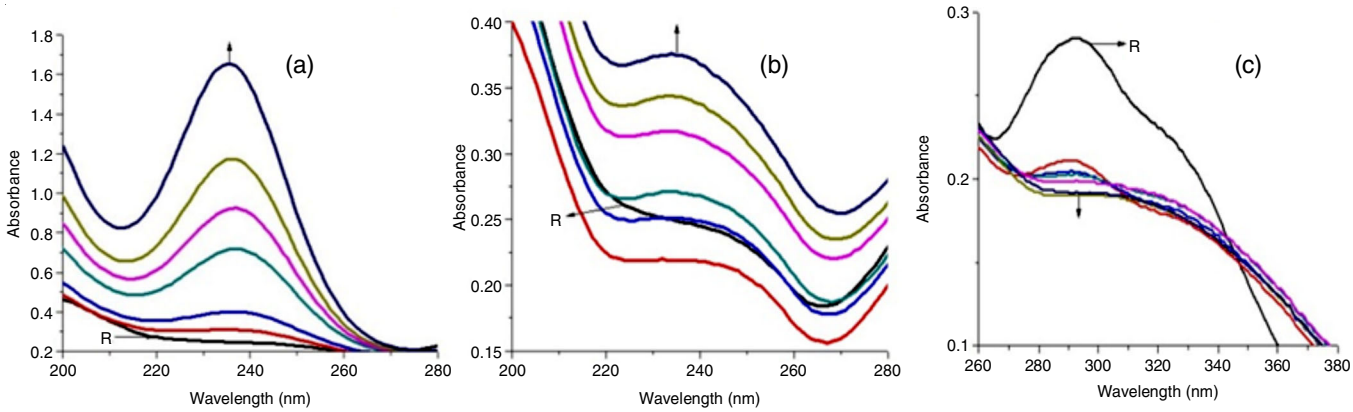

Fig. 5. Development of new peak for the addition of metal ion of (a) Hg (b) Pb and (c) Ni

UV-visible spectral titration studies were carried out by taking 2.5 mL of 1×10^{-5} M receptor solution in the cuvette and then adding 20 µL aliquot of 1.25×10^{-3} M metal(II) salt solutions. The overall spectral swap noticed for the addition of Cu^{2+} ions (Fig. 4a) along with the formation of metal-to-ligand charge transfer band responsible for the combination of metal ions with receptor [5] is shown around 460 nm (Fig. 4b) and redshift of 295 nm peaks to 311 nm (Fig. 4c) clearly exposes the binding aptitude of compound R1 towards Cu^{2+} ions.

Cumulative addition of Hg^{2+} and Pb^{2+} generate a new peak around 235 nm (Fig. 5a) and 234 nm (Fig. 5b), respectively. Successive addition of Ni^{2+} convert the 292 nm peak of receptor in to a broad shoulder in the same wavelength region (Fig. 5c). Minimum changes were observed for the addition of Cd^{2+} and Mn^{2+} ions.

The n-π* transition in compound R2 might have gone well due to the presence of electron donating methyl groups and have caused display of a prominent peak around 335 nm (Fig. 6). Like compound R1, compound R2 also exposes MLCT absorption peak for copper ion (Fig. 7a). Addition of mercury ions generate prominent peak around 236 nm (Fig. 7b) and transformation of 300 nm shoulder to a peak at 298 nm (Fig. 7c) is observed for the successive addition of lead.

Sensing aptitude using cyclic voltammetry: To ascertain the binding priority order of various metal ions, electrochemical responses for the applied potential were recorded. The voltammograms of metal free R1 (Fig. 8a-b) with different scan rate

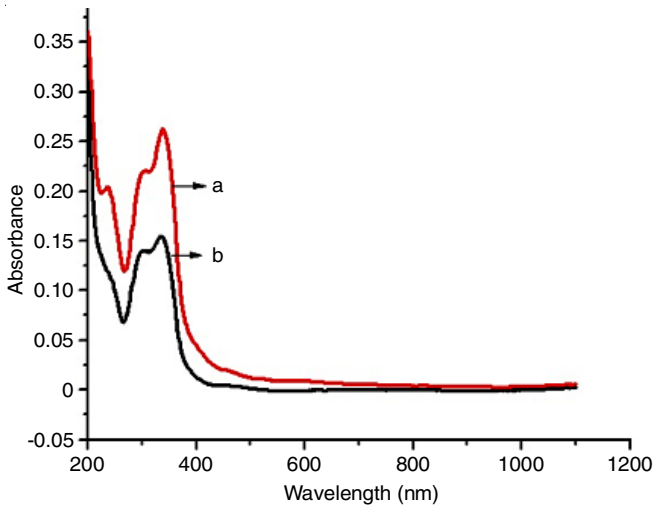

Fig. 6. Electronic spectra of R2 in (a) ethanol (b) acetonitrile

pertained with increasing ΔE_P, I_{pa} and I_{pc} values (Table-1) and magnified observed ΔE_P (73-120 mV instead of 59 mV) highlighted that a quasi-reversible one-electron redox process [32].

Appropriate salts of metal cations titration by taking 10 mL of R1 solution (1×10^{-3} M) and then adding either 1×10^{-3} M (Fig. 9a) or 1×10^{-1} M (Fig. 9b) metal salt solution up to seven equivalents produce voltammogram with positive potential shift for oxidation peak and negative potential shift for reduction peak that advocate electrochemical sensing of metal ions [33-35].

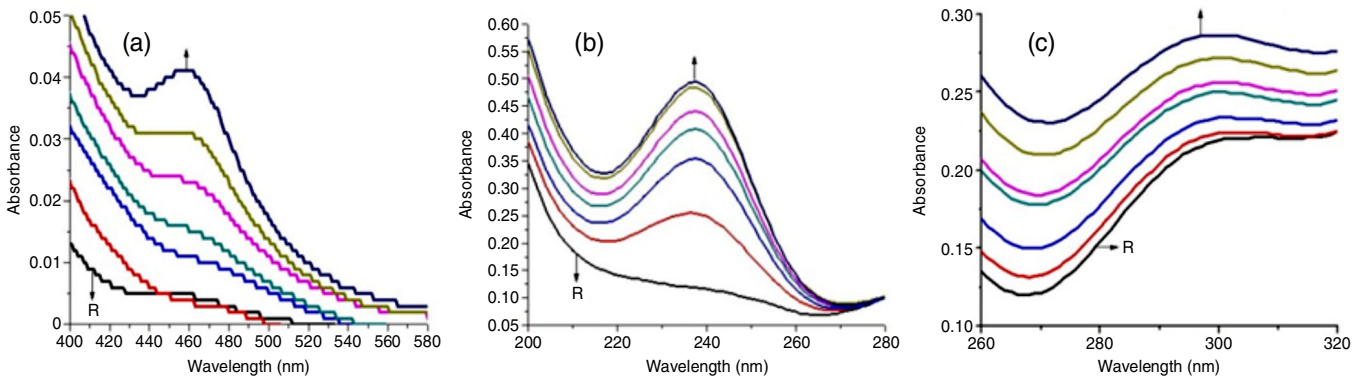

Fig. 7. Formation of pre-eminent peaks in the spectrum of R2 for the addition (a) Cu^{2+} ions (b) Hg^{2+} ions and (c) Pb^{2+} ions

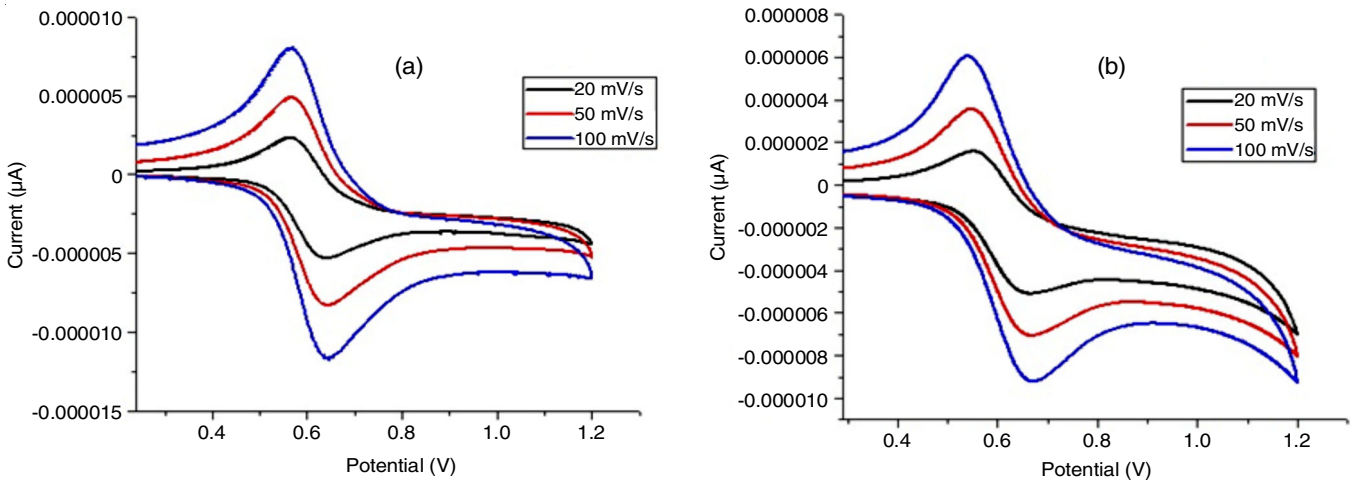

Fig. 8. Voltammograms of R1 (1×10^{-3} M) in (a) acetonitrile (b) ethanol

TABLE-1
ELECTROCHEMICAL DATA OF R1 (10^{-3} M)

Scan rate (mV/s)	Solvent-acetonitrile						Solvent-ethanol					
	E_{pa} (V)	E_{pc} (V)	ΔE_p (V)	$E_{1/2}$ (V)	$I_{pa} \times 10^{-6}$ (μA)	$I_{pc} \times 10^{-6}$ (μA)	E_{pa} (V)	E_{pc} (V)	ΔE_p (V)	$E_{1/2}$ (V)	$I_{pa} \times 10^{-6}$ (μA)	$I_{pc} \times 10^{-6}$ (μA)
20	0.639	0.563	0.076	0.601	-5.295	2.363	0.659	0.553	0.105	0.606	-5.109	1.619
50	0.641	0.568	0.073	0.604	-8.273	4.928	0.666	0.545	0.120	0.606	-7.066	3.558
100	0.641	0.565	0.076	0.603	-11.737	8.049	0.666	0.538	0.127	0.602	-9.278	6.044

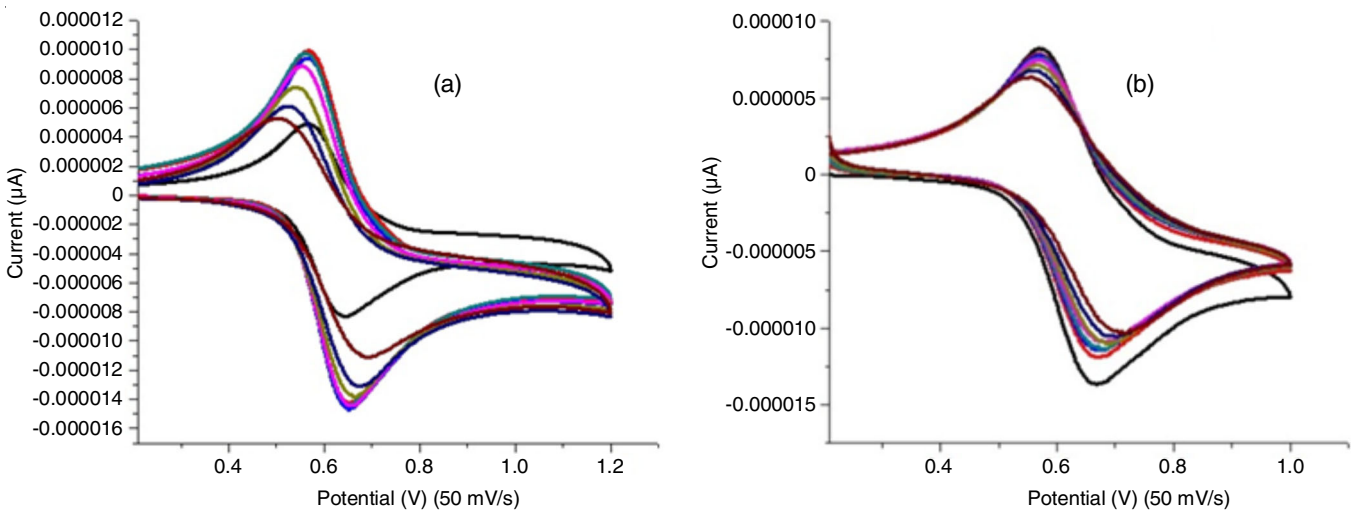

Fig. 9. CV titration study of R1 (10^{-3} M) with different concentration of Cu^{2+} ion (a) 10^{-3} M (b) 10^{-1}M

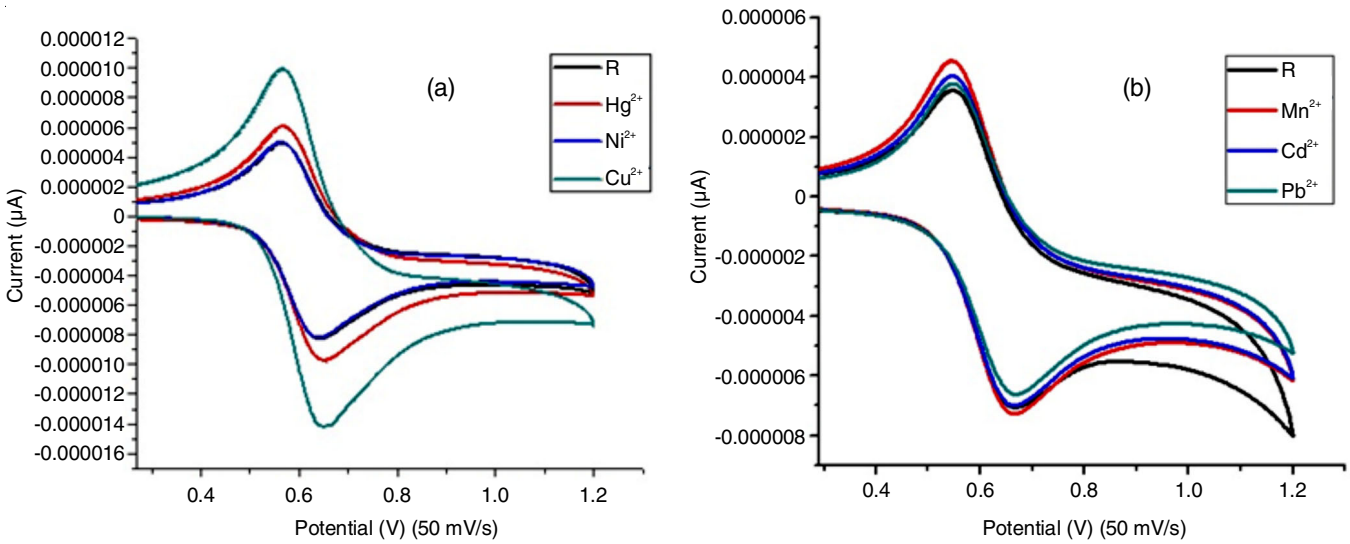

Fig. 10. Cyclic voltammograms observed for the addition of different metal ion (10^{-3} M) with R1 (10^{-3}M) in a) acetonitrile (b) ethanol

TABLE-2
CV TITRATION DATA FOR R1 (10^{-3} M) WITH DIFFERENT METAL ION HAVING 10^{-3} M CONCENTRATION

Addition	E_{pa} (V)	E_{pc} (V)	ΔE_p (V)	$E_{1/2}$ (V)	$I_{pa} \times 10^{-6}$ (μA)	$I_{pc} \times 10^{-6}$ (μA)
Solvent-acetonitrile						
R1	0.641	0.568	0.073	0.604	-8.273	4.928
Hg^{2+}	0.651	0.568	0.083	0.609	-9.751	6.044
Cu^{2+}	0.649	0.568	0.081	0.608	-14.295	9.882
Ni^{2+}	0.644	0.565	0.078	0.604	-8.154	4.920
Solvent-ethanol						
R1	0.666	0.545	0.120	0.606	-7.066	3.558
Cd^{2+}	0.668	0.548	0.120	0.608	-6.963	4.080
Mn^{2+}	0.663	0.545	0.117	0.604	-7.227	4.605
Pb^{2+}	0.663	0.548	0.115	0.606	-6.610	3.838

Cyclic voltammograms recorded for various metal ion solutions having 10^{-3} M concentration are presented in Fig. 10. The observed ΔE_P value of them falls between 73-120 mV. Further, the variation noticed in the decreased amount of Ipa (Table-2), exposes the change in ability of binding and also the repulsion between the oxidized ferrocene unit and bonded metal ion [35].

Fig. 11 represents the percentage decrease in change of current (ΔI_{pa}) calculated from the anodic current (I_{pa}) and sensing order for compound R1 to various metal ion as Cu (72.8) > Hg (17.8) > Pb (6.4) > Mn(2.3) > Cd(1.5) > Ni(1.4).

For 10^{-1} M concentration of metal salt solution, the ΔI_{pa} value calculated for the oxidation wave (Table-3) throw back binding power of compound R1 towards the various metal ion (Fig. 11) as Ni (24.6) > Mn (22.2) > Pb (17.5) > Cu (13.1) > Hg (2.6) > Cd (2.1). Non-identical order of arrangement with respect to metal ion concentration assemblage disclose that compound R1 is capable sensing Cu^{2+}, Hg^{2+} and Pb^{2+} ions even at lower concentration and at higher concentration level proficient headed for Ni^{2+}, Mn^{2+}, Pb^{2+} and Cu^{2+}.

Electrochemical studies of compound R2 display two redox peaks (Fig. 12a-b) with all different scan rate. The peak witnessed around 0.63 V is accountable for Fe(II)/Fe(III) and other observed around 0.89 V may be assigned for electron transition among azomethine group and aromatic moiety of receptor [32].

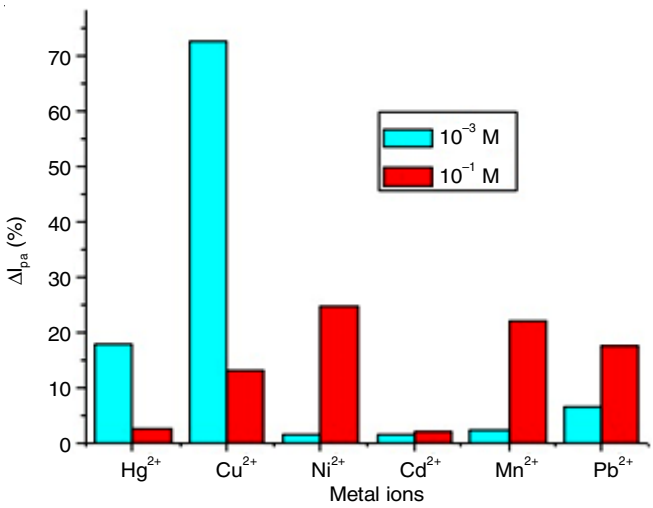

Fig. 11. Comparision of concentrations required for sensing of R1

Titration studies: Results obtained in titration studies by adopting the same procedure used for compound R1 under different concentration of metal ion (Fig. 13a-b) illustrates the sensing behaviour of compound R2. The disappearance of reduction peak, allocated for electron transition, after fourth addition of Cu^{2+} ion ascertain the metal ion coordination with azomethine group [32].

TABLE-3
CV TITRATION DATA FOR R1 (10^{-3} M) WITH DIFFERENT METAL IONS HAVING 10^{-1} M CONCENTRATION

Addition	E_{pa} (V)	E_{pc} (V)	ΔE_p (V)	$E_{1/2}$ (V)	$I_{pa} \times 10^{-6}$ (μA)	$I_{pc} \times 10^{-6}$ (μA)
Solvent-acetonitrile						
R1	0.641	0.568	0.073	0.604	-8.273	4.928
Hg^{2+}	0.670	0.571	0.098	0.621	-1.328	9.033
Cu^{2+}	0.669	0.570	0.099	0.620	-1.184	7.854
Ni^{2+}	0.674	0.575	0.098	0.625	-1.027	5.927
Solvent-ethanol						
R1	0.666	0.545	0.120	0.606	-7.066	3.558
Cd^{2+}	0.682	0.540	0.142	0.611	-9.141	5.147
Mn^{2+}	0.699	0.529	0.169	0.614	-6.956	3.866
Pb^{2+}	0.675	0.537	0.138	0.606	-7.380	4.334

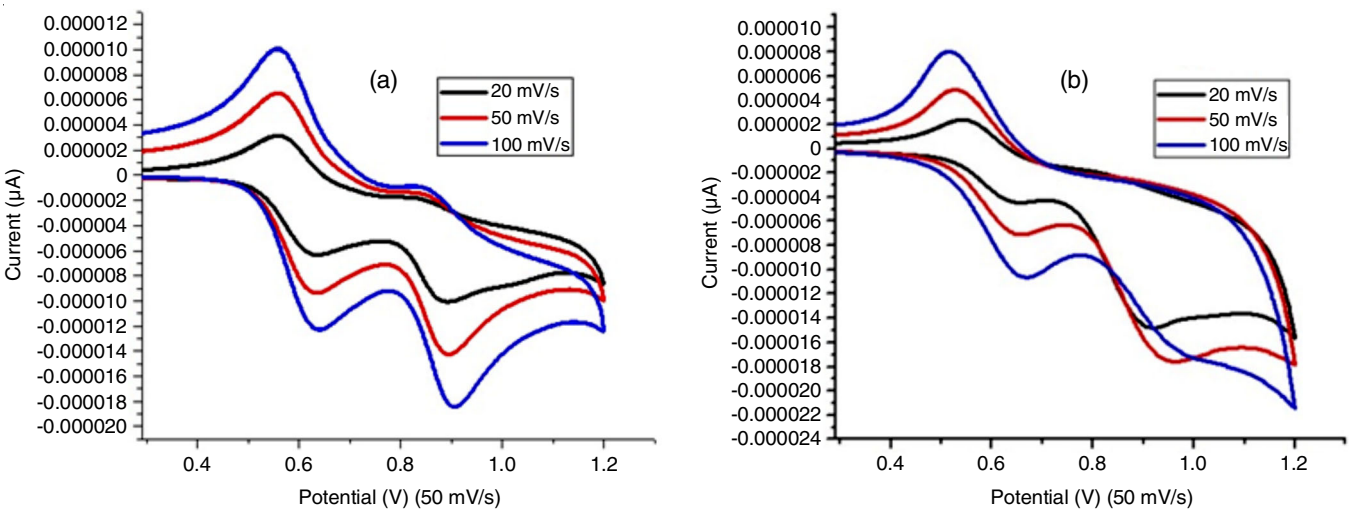

Fig. 12. Cyclic voltammetric curves of R2 with different sweep rate in (a) acetonitrile (b) ethanol

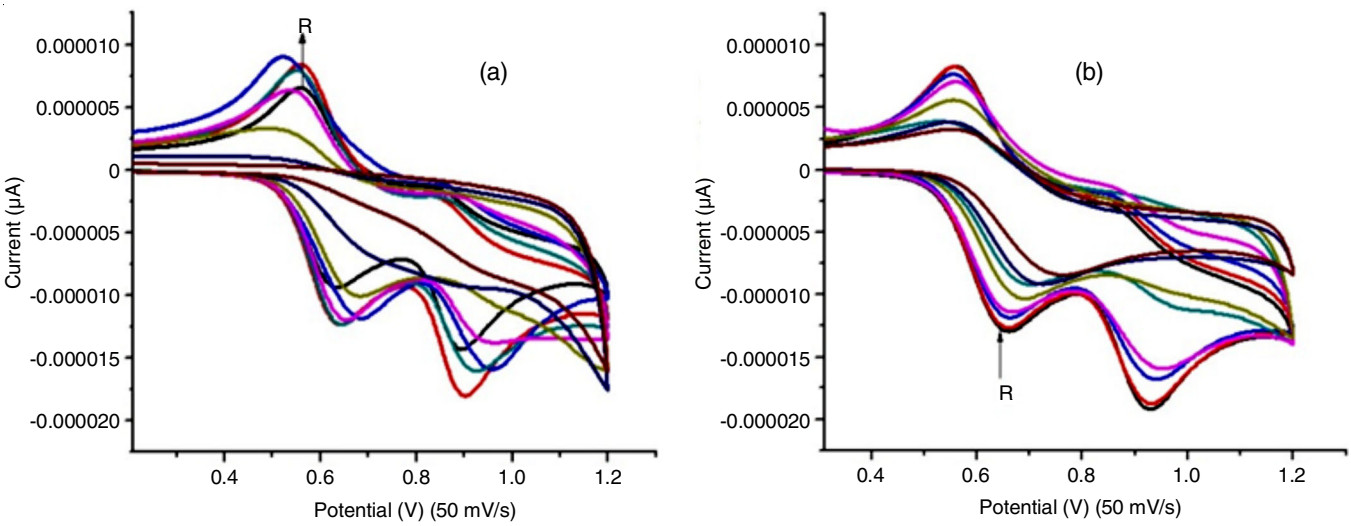

Fig. 13. Change in cyclic voltammogram of R2 for the addition Cu^{2+} ions (a) 10^{-3} M (b) 10^{-1} M

Fig. 14 represents the voltammograms recorded for the addition (20 μL) of various metal ion solutions (10^{-3} M) to receptor solution (10^{-3} M) in acetonitrile and ethanol solvents. Variation noticed in the decreased amount of I_{pa} (Table-4) exposes the change in ability of the receptor to bind with different metal ion. The disappearance of the oxidation peak responsible for electron transition associated with azomethine group after the addition of metal ions (Fig.14b) with magnified ΔE_p values (131-149 mV) also confirmed the effective coordination of metal ions with receptor.

Based on the ΔI_{pa} values, the response trend of compound R2 (Fig. 15) at lower concentration of metal ion is in the order of Cu (86.93) > Ni (26.13) > Mn (20.11) > Cd (19.36) > Pb (1.01) > Hg (0.68) and for higher concentration it is Ni (87.21) > Cu (86.54) > Pb (30.7) > Hg (26.21) > Mn (22.7) > Cd (17.08) (Table-4). Above trend indicates that compound R2 is

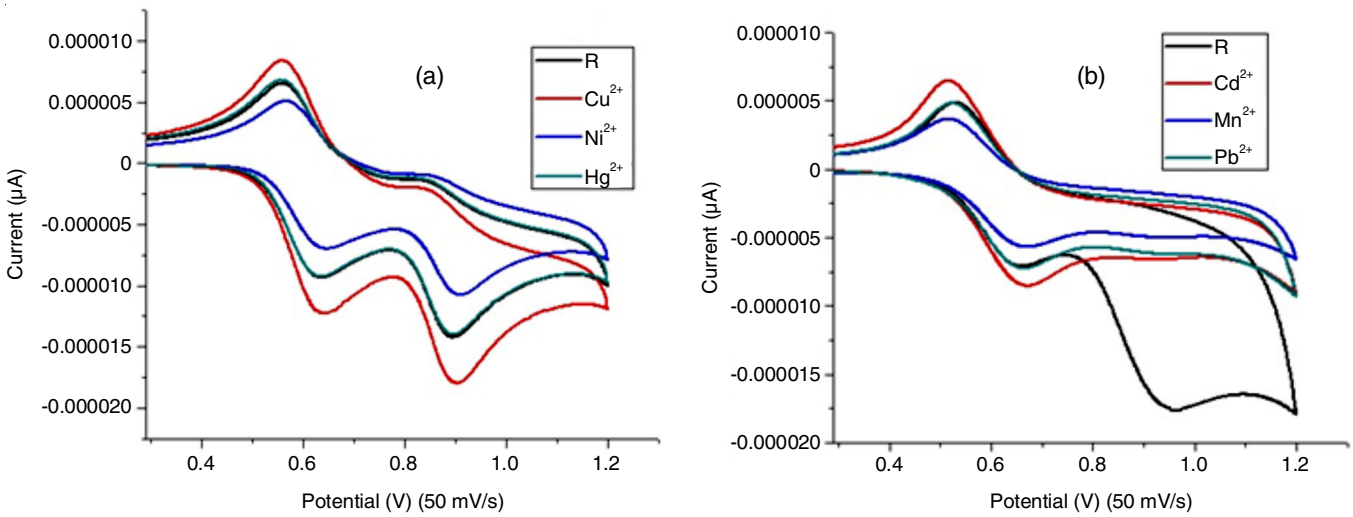

Fig. 14. Cyclic voltammograms recorded for the addition of different metal ion (10^{-3}M) with R2 (10^{-3} M) in (a) acetonitrile (b) ethanol

TABLE-4
CV TITRATION DATA FOR R2 WITH DIFFERENT METAL IONS HAVING 10^{-3}M CONCENTRATION

Addition	E^1_{pa} (V)	E^1_{pc} (V)	ΔE^1_p (V)	$E^1_{1/2}$ (V)	$I^1_{pa} \times 10^{-6}$ (μA)	$I^1_{pc} \times 10^{-6}$ (μA)
Solvent-acetonitrile						
R2	0.632	0.559	0.073	0.596	-9.443	6.548
Hg^{2+}	0.635	0.557	0.078	0.596	-9.379	6.822
Cu^{2+}	0.632	0.559	0.073	0.596	-9.443	6.548
Ni^{2+}	0.644	0.563	0.080	0.604	-6.975	5.040
Solvent-ethanol						
R2	0.657	0.525	0.131	0.591	-7.137	4.870
Cd^{2+}	0.668	0.514	0.153	0.591	-8.519	6.463
Mn^{2+}	0.666	0.519	0.146	0.592	-5.701	3.637
Pb^{2+}	0.668	0.521	0.149	0.596	-7.209	4.870

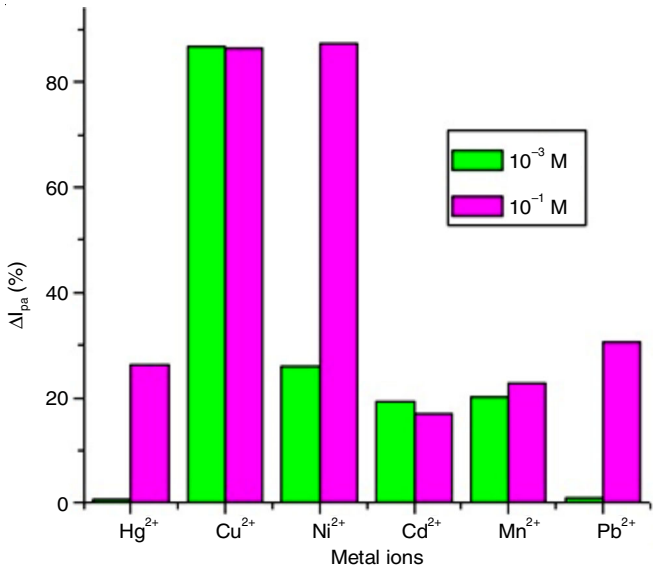

Fig. 15. Comparison of concentrations of metal ions required for sensing of R2

capable of sensing even at the trace amount of Cu^{2+} and Ni^{2+} whereas higher amount of Hg^{2+} and Cd^{2+} are required for detection.

Antimicrobial studies: The antibacterial activity with Mueller-Hinton agar base for synthesized receptors R1 and R2 was discovered against selected microbial *viz*. *Staphylococcus aureus*, *streptococcus faecalis*, *Escherichia coli* and *Salmonella typhimurium*, by disc diffusion method. Similarly, antifungal studies were carried out with Sabouraud's Dextrose agar as base for *Aspergillus niger* and *Candida albicans*. The results tabulated for antibacterial studies were at par with standard ciprofloxacin except for *Streptococcus faecalis* which showed no zone of inhibition (Table-5). Fungi *Aspergillus niger* growth is prevented strongly (nearly 67%) compared to the standard ketoconazole, which is abnormal and highly useful to manhood as limited antifungal agents are available [24].

Molecular docking studies: In order to support the antimicrobial activity exhibited by the synthesized compounds, it was subjected to docking with respective protein of the bacteria and fungi (1PTF-*Streptococcus faecalis*, 6KVQ-*Staphylococcus aureus*, 7BU2-*Escherichia coli*, 4YXB-*Salmonella typhimurium*, 3K4Q-*Aspergillus niger*, 6TZ6-*Candida albicans*) and the docking results are given in Table-6. The 3D & 2D view binding of ligand R1& R2 are presented in Fig. 16a-f. Both compounds showed binding energy to the target protein site with the binding scores between -4.63 to -8.81 Kcal mol^{-1}. Compounds R1 and R2 showed the highest binding score with protein 3K4Q which is the enzyme for microbes *Aspergillus niger*. *in vitro* studies of compounds R1 and R2 exhibited inhibition band of 10 mm and 11 mm against *E. coli* and this result is supported in the docking with the score of -7.57 and -8.53 Kcal mol^{-1} with the enzyme 7BU2 present in *E. coli*.

TABLE-5
DATA ARRIVED FOR R1 & R2 IN ANITIMICROBIAL *in vitro* STUDIES

Microorganism	Control (negative)	Zone of inhibition (mm)		Ciprofloxacin/ Ketoconazole
		R1	R2	
Bacteria				
Staphylococcus aureus	–	9	9	35
Streptococcuse faecalis	–	–	–	28
Escherichia coli	–	10	11	35
Salmonella typhimurium	–	5	–	30
Fungi				
Aspergillus niger	–	10	–	15
Candida albicans	–	–	–	27

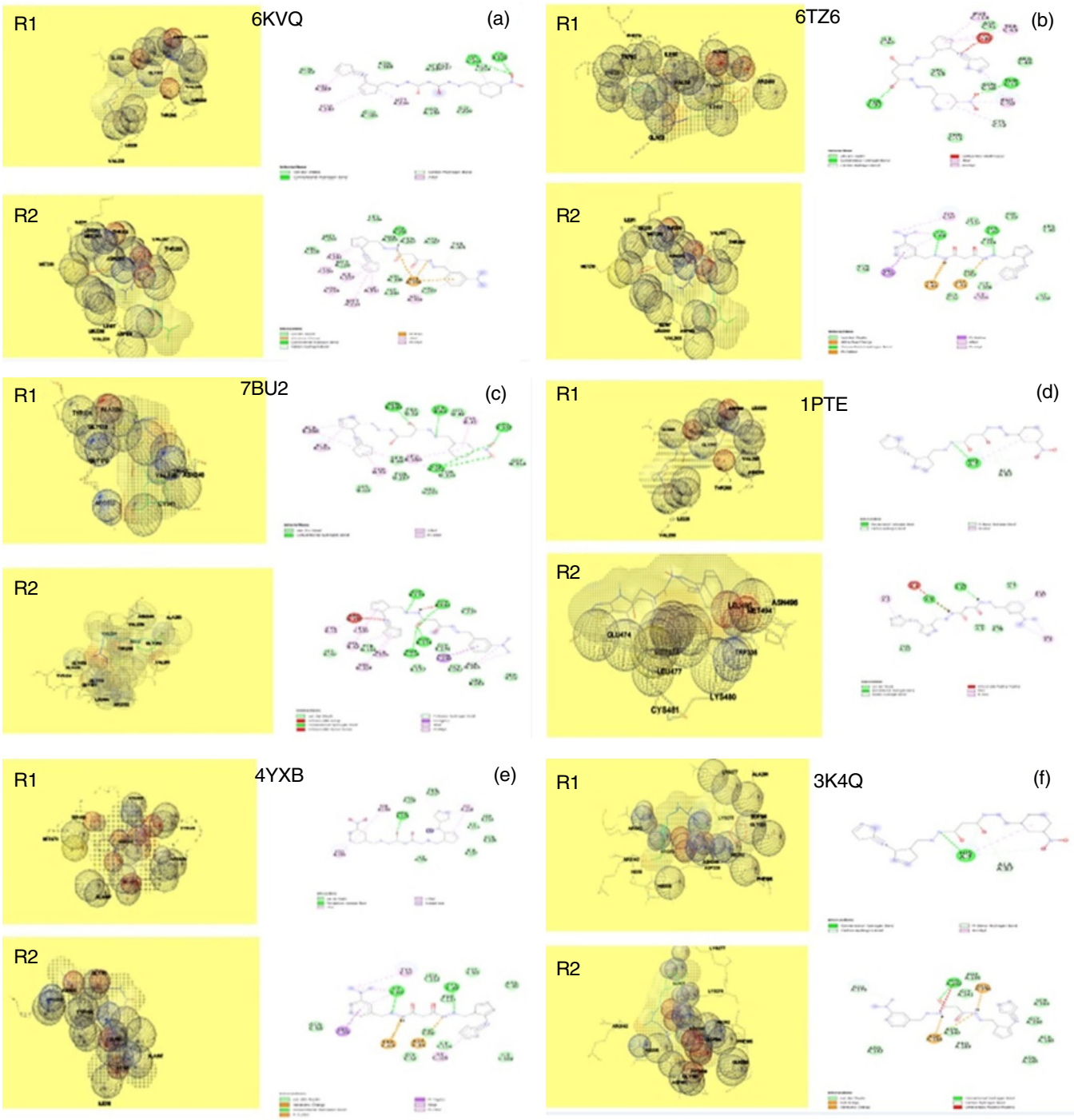

Fig. 16. Docked 3D and 2D view of R1 and R2 with a) 6KVQ b) 6TZ6 c) 7BU2 d) 1PTF e) 4YXB and f) 3K4Q

TABLE-6
DOCKING SCORE OF R1 & R2 WITH THE PROTEINS OF BACTERIA AND FUNGI

Compd. code	PDB	Free binding energy (kcal mol^{-1})	Hydrogen bonds with receptor amino acids	Distance (Å)
R1	6KVQ	-6.97	188-ASN	3.7
			192-GLN	3.76
			228-ILE	3.69
			243-LYS	3.41
			249-LEU	3.12
R2	6KVQ	-8.57	197-ILE	3.16
			199-ASP	3.39
			200-LEU	3.17
			203-VAL	3.27
			209-LEU	3.8
			214-VAL	3.94
			261-LEU	3.38
			309-THR	3.5
R1	6TZ6	-8.6	30-TYR	3.93
			50-PHE	3.69
			59-VAL	3.88
			60-ILE	3.98
			114-PHE	3.23
R2	6TZ6	-7.27	40-PHE	3.58
			41-ASP	3.93
			59-VAL	3.73
			60-ILE	3.45
			97-TYR	4
			105-ILE	3.36
			114-PHE	3.58
R1	7BU2	-7.57	52-TRP	3.67
			91-TRP	3.49
			156-THR	3.98
			180-LEU	3.74
			286-ALA	3.3
			287-THR	3.09
R2	7BU2	-8.53	180-LEU	3.47
			236-VAL	3.43
			240-ASN	3.58
			324-VAL	3.43
			329-ALA	2.98
			332-ARG	3.99
R1	1PTF	-4.63	5-GLU	3.4
			6-PHE	3.45
			7-HIS	1.84
			60-ASP	4.85
R2	1PTF	-6.97	3-LYS	3.55
			7-HIS	3.96
			87-ALA	3.65
R1	4YXB	-6.07	194-TYR	3.18
			195-LEU	3.89
			214-ASP	3.97
			216-ILE	3.64
R2	4YXB	-7.24	26-ALA	3.67
			29-PRO	3.78
			46-ILE	3.27
			53-ILE	3.43
			194-TYR	3.92
R1	3K4Q	-8.81	68-LYS	3.97
			338-HIS	3.24
			339ASP	3.95
R2	3K4Q	-8.21	179-GLU	3.39
			282-HIS	2.83
			340	2.92

Conclusion

To overcome the challenges in synthesizing the Schiff bases with the mixture of aromatic aldehyde con-taining ferrocene carboxaldehyde and its derivatives as one of the component, attempts made by our research group resulted with unsymmetrical Schiff bases N'^{1}-((*E*)-ferrocenylidene)-N'^{3}-((*E*)-4-nitrobenzylidene)malonohydrazide and N'^{1}-((*E*)-ferrocenylidene)-N'^{3}-((*E*)-4-*N*,*N*-dimethylaminobenzylidene)-malonohydrazide. FTIR, ^{1}H NMR and mass spectral analysis data substantiate the formation of above compounds. Potentiality in multi-metal ion sensing is identified by electronic spectral studies. Role of concentration of receptor and metal ions is brought in to attention by estimating the ΔI_{pa} calculated values. Antimicrobial studies and molecular docking studies revealed that synthesized compounds inhibit more efficiently fungi rather than bacteria.

ACKNOWLEDGEMENTS

The authors acknowledge the support from Prof. K. Pandian, Controller of Examinations, University of Madras, Chennai, India for the UV-Visible spectral studies. One of the authors, (DS) thanks State Government of Tamil Nadu, India for the annual research assistant grant.

CONFLICT OF INTEREST

The authors declare that there is no conflict of interests regarding the publication of this article.

REFERENCES

1. L. Eddaif, A. Shaban and J. Telegdi, *Int. J. Environ. Anal. Chem.*, **99**, 824 (2019); https://doi.org/10.1080/03067319.2019.1616708
2. J. Dalmieda and P. Kruse, *Sensors*, **19**, 5134 (2019); https://doi.org/10.3390/s19235134
3. B. Bansod, T. Kumar, R. Thakur, S. Rana and I. Singh, *Biosens. Bioelectron.*, **94**, 443 (2017); https://doi.org/10.1016/j.bios.2017.03.031
4. Y. Lu, X. Liang, C. Niyungeko, J. Zhou, J. Xu and G. Tian, *Talanta*, **178**, 324 (2018); https://doi.org/10.1016/j.talanta.2017.08.033
5. R. Pandey, R.K. Gupta, M. Shahid, B. Maiti, A. Misra and D.S. Pandey, *Inorg. Chem.*, **51**, 298 (2012); https://doi.org/10.1021/ic201663m
6. A.M. Abu-Dief and I.M. Mohamed, *Beni-Suef Univ. J. Basic Appl. Sci.*, **4**, 119 (2015); https://doi.org/10.1016/j.bjbas.2015.05.004
7. A.L. Berhanu, I. Gaurav, I. Mohiuddin, A.K. Malik, J.S. Aulakh, V. Kumar and K.-H. Kim, *TrAC-Trends Analyt. Chem.*, **116**, 74 (2019); https://doi.org/10.1016/j.trac.2019.04.025
8. J.J. Lee, Y.W. Choi, G.R. You, S.Y. Lee and C. Kim, *Dalton Trans.*, **44**, 13305 (2015); https://doi.org/10.1039/C5DT00957J
9. F. Oton, A. T'arraga, M.D. Velasco and P. Molina, *Dalton Trans.*, **7**, 1159 (2005); https://doi.org/10.1039/B419082C
10. Y. Fang, Y. Zhou, Q. Rui and C. Yao, *Organometallics*, **34**, 2962 (2015); https://doi.org/10.1021/acs.organomet.5b00285
11. H. Jiqu and Y. Qixia, *Spectrochim. Acta A Mol. Biomol. Spectrosc.*, **149**, 487 (2015); https://doi.org/10.1016/j.saa.2015.04.075
12. E. Denkhaus and K. Salnikow, *Crit. Rev. Oncol. Hematol.*, **42**, 35 (2002); https://doi.org/10.1016/S1040-8428(01)00214-1

13. X. Qi, E.J. Jun, L. Xu, S.-J. Kim, J.S. Joong Hong, Y.J. Yoon and J. Yoon, *J. Org. Chem.*, **71**, 2881 (2006); https://doi.org/10.1021/jo052542a
14. P.G. Georgopoulos, A. Roy, M.J. Yonone-Lioy, R.E. Opiekun and P.J. Lioy, *J. Toxicol. Environ. Health B*, **4**, 341 (2001); https://doi.org/10.1080/109374001753146207
15. A.C. Rosenzweig and T.V. O'Halloran, *Curr. Opin. Chem. Biol.*, **4**, 140 (2000); https://doi.org/10.1016/S1367-5931(99)00066-6
16. E. Gaggelli, H. Kozlowski, D. Valensin and G. Valensin, *Chem. Rev.*, **106**, 1995 (2006); https://doi.org/10.1021/cr040410w
17. G. Jiang, L. Xu, S. Song, C. Zhu, Q. Wu, L. Zhang and L. Wu, *Toxicology*, **49**, 244 (2008); https://doi.org/10.1016/j.tox.2007.10.028
18. M. Aschner, T.R. Guilarte, J.S. Schneider and W. Zheng, *Toxicol. Appl. Pharmacol.*, **221**, 131 (2007); https://doi.org/10.1016/j.taap.2007.03.001
19. L.G. Strause, J. Hegenauer, P. Saltman, R. Cone and D. Resnick, *J. Nutr.*, **116**, 135 (1986); https://doi.org/10.1093/jn/116.1.135
20. J. Crossgrove and W. Zheng, *NMR Biomed.*, **17**, 544 (2004); https://doi.org/10.1002/nbm.931
21. O. Sunnapu, N.G. Kotla, B. Maddiboyina, S. Singaravadivel and G. Sivaraman, *RSC Advances*, **6**, 656 (2016); https://doi.org/10.1039/C5RA20482H
22. G.V.C. Tamil Selvan, V.M.V.E. Israel and P.M. Selvakumar, *New J. Chem.*, **42**, 902 (2018); https://doi.org/10.1039/C7NJ03888G
23. D. Sinha, A.K. Tiwari, S. Singh, G. Shukla, P. Mishra, H. Chandra and A.K. Mishra, *Eur. J. Med. Chem.*, **43**, 160 (2008); https://doi.org/10.1016/j.ejmech.2007.03.022
24. M.M. Azevedo, R. Teixeira-Santos, A.P. Silva, L. Cruz, E. Ricardo, C. Pina-Vaz and A.G. Rodrigues, *Front. Microbiol.*, **6**, 669 (2015); https://doi.org/10.3389/fmicb.2015.00669
25. N. Tazin, V.D. Ragole and D.S. Wankhede, *Inorg. Nano-Metal Chem.*, **49**, 291 (2019); https://doi.org/10.1080/24701556.2019.1661449
26. C.F. Bagamboula, M. Uyttendaele and J. Debevere, *Food Microbiol.*, **21**, 33 (2004); https://doi.org/10.1016/S0740-0020(03)00046-7
27. G.M. Morris, R. Huey, W. Lindstrom, M.F. Sanner, R.K. Belew, D.S. Goodsell and A.J. Olson, *J. Comput. Chem.*, **30**, 2785 (2009); https://doi.org/10.1002/jcc.21256
28. T.P. Gryaznova, S.A. Katsyuba, V.A. Milyukov and O.G. Sinyashin, *J. Organomet. Chem.*, **695**, 2586 (2010); https://doi.org/10.1016/j.jorganchem.2010.08.031
29. M.C. Mandewale, B. Thorat, Y. Nivid, R. Jadhav, A. Nagarsekar and R. Yamgar, *J. Saudi Chem. Soc.*, **22**, 218 (2016); https://doi.org/10.1016/j.jscs.2016.04.003
30. B. Catikkas, *Period. Eng. Nat. Sci.*, **5**, 237 (2017); https://doi.org/10.21533/pen.v5i2.139
31. R. Benramdane, F. Benghanem, A. Ourari, S. Keraghel and G. Bouet, *J. Coord. Chem.*, **68**, 560 (2015); https://doi.org/10.1080/00958972.2014.994514
32. P. Kamatchi, S. Selvaraj and M. Kandaswamy, *Polyhendron*, **24**, 900 (2005); https://doi.org/10.1016/j.poly.2005.02.012
33. M. Li and R. Wang, *IOP Conf. Series Earth Environ. Sci.*, **61**, 012043 (2017); https://doi.org/10.1088/1755-1315/61/1/012043
34. M. Alfonso, A. Tarraga and P. Molina, *Dalton Trans.*, **39**, 8637 (2010); https://doi.org/10.1039/C0DT00450B
35. A. Kamal, S. Kumar, V. Kumar and R.K. Mahajan, *Sens. Actuators B Chem.*, **221**, 370 (2015); https://doi.org/10.1016/j.snb.2015.06.147